

IGNITION OF PREMIXED HYDROGEN/AIR BY HEATED COUNTERFLOW

X. L. ZHENG,¹ J. D. BLOUCH,¹ D. L. ZHU,¹ T. G. KREUTZ² AND C. K. LAW¹

¹*Department of Mechanical and Aerospace Engineering*

²*Center for Energy and Environmental Studies*

Princeton University

Princeton, NJ 08544, USA

The inert temperature required to ignite a lean premixed hydrogen/air mixture in a counterflow was determined experimentally and numerically using detailed chemistry and transport. It was found that above $\phi = 0.2$, the ignition temperatures increased with increasing equivalence ratio. This effect is due to the fact that the ignition kernel is located on the hot, inert side of the flow and preferential diffusion of hydrogen makes the flow self-stratifying, resulting in a rich mixture in the ignition kernel even for a very lean free-stream mixture. The dearth of O_2 in the kernel reduces the reaction rates to the point where diffusive loss becomes significant relative to the rates of kinetic production and consumption. In the presence of this significant transport loss mechanism, premixed ignition temperatures are much higher than non-premixed ignition temperatures and the influence of the strain rate is likewise increased. Adding a few percent of O_2 to the hot inert side of the flow lowers the kernel equivalence ratio and increases the reaction rates to the point where diffusive effects are no longer of the same order as kinetic effects. In these cases, the ignition temperatures drop significantly to values close to those of non-premixed ignition even though the free-stream flow is still predominantly premixed.

Introduction

Recently, a series of computational and experimental investigations [1–9] have been conducted on the forced ignition of a cold hydrogen jet by a counterflowing heated air jet. These studies yielded the interesting result [5,6] that the ignition characteristics in this convective-diffusive system qualitatively mimic the homogeneous system, in that the ignition boundary in terms of the system pressure and temperature follows closely the Z-shaped explosion limits of homogeneous hydrogen/oxygen mixtures. The effect of aerodynamic straining is simply a displacement of the Z-curve along the line of the crossover temperature, with the result that, for a given pressure, the ignition temperatures in the second limit are remarkably insensitive to the strain rate. Additional exploration revealed that, in this limit, ignition is induced through radical instead of thermal runaway, and consequently, the ignition state can be numerically reproduced by suppressing the heat-release terms in the conservation equations. Indeed, since the hydrogen/oxygen system is so chemically reactive, the rates of the key elementary reactions are several orders faster than those of convection and diffusion such that kinetically controlled ignition events were also observed for some first- and third-limit situations that are close to the second limit. Mechanistically, the results above were interpreted

on the basis of ignition occurring in an ignition kernel situated in the hot region of the flow that contains peaks of both reaction rates and the key intermediate species.

While the results above are fundamentally interesting and technically important, many practical situations exist in which the ignition of a premixture is of relevance. Examples include the initiation of accidental explosions of a premixed combustible and ignition in the mixing layer of the hot recirculation zone for flame holding. Furthermore, within turbulent flames there are pockets of unburned combustibles that could be ignited by the hot combustion products. While our studies have shown that non-premixed ignition exhibits features of homogeneous systems, we are also confronted by the fact that the structure and response of non-premixed and premixed flames are qualitatively different. It is therefore of interest to extend our studies on non-premixed ignition to premixed ignition in order to identify the differences and similarities between the two systems.

The above-mentioned considerations constituted the initial motivation for the present research, which was to determine the state of ignition, and the associated characteristics, for a premixed hydrogen/air jet by a heated counterflowing inert jet. The phenomena turned out to be substantially richer than

anticipated, embodying new understandings on ignition that are unique to the premixed system, while providing unifying concepts for non-premixed and premixed ignition. In particular, we shall show, in due course, that, because of diffusional stratification and hence de-mixing of the mixture composition, premixed ignition could be more difficult than non-premixed ignition. However, such a difficulty can be partly mitigated by doping the inert with a small quantity of oxygen, which in effect is instilling a non-premixed character to the system. The resulting partially premixed system then constitutes the needed transition between nonpremixed and premixed ignition. We note in passing that Vlachos et al. [10] computationally investigated the ignition of a premixed hydrogen/air jet by a hot stagnation surface, providing useful insight into the thermal and chemical characteristics of the various bifurcated states representing ignition. Since the stagnation surface is not permeable in this study [10], as compared with that offered by the impinging jet, the concentration stratification mechanism that is responsible for the phenomena investigated herein is basically absent.

In the following, the experimental and computational methodologies will be discussed first. This will be followed by examining effects of the mixture equivalence ratio (ϕ), strain rate, and preferential diffusion. Finally, oxygen addition to the hot, inert side of the flow will be investigated.

Experimental and Computational Methodology

The burner used in non-premixed ignition experiments [4] was adapted for the present study. The upper part of the counterflow was formed by a nitrogen or nitrogen/oxygen jet from a 20 mm diameter quartz tube, while the lower part was a hydrogen/air mixture issuing from a 10 mm bronze tube. The tubes were separated by 20 mm and were surrounded by nitrogen coflows. A silicon carbide heater was placed in the upper flow and the temperature was regulated using a proportional-integral-derivative temperature controller. The entire burner tube assembly was contained within a pressure chamber filled with nitrogen. Temperature and velocity fields in the axial direction between the burner tubes were respectively measured by a bare K-type thermocouple (0.003 in. diameter wire) and a two-component laser Doppler velocimetry (LDV) system.

Unlike experiments with non-premixed ignition, the burner geometry and experimental conditions were restricted by the need to avoid flashback, which could be a serious problem with hydrogen because of its high burning rate. High flow rates are therefore needed to stabilize the flame within the flow field upon ignition, although they cannot be so high as to

undergo transition to turbulence. To extend the experimental conditions to the highest possible ϕ for the present lean mixtures, and since the reactant flow has the higher Reynolds number of the two jets because of its lower temperature and thereby kinematic viscosity, the diameter of the lower burner tube was reduced to avoid the transition to turbulence.

Data were collected in flows with the stagnation surface near the mid-point of the flow field. The hot boundary temperature was slowly increased until a flame appeared. The hydrogen flow was doped with a trace amount of methane so that ignition could be identified visually. Some experiments were repeated without methane, and ignition was confirmed by passing a wire through the flame region and checking whether it glowed. Before measuring the temperature of the hot boundary at this ignition state, it was necessary to extinguish the flame by reducing the fuel concentration so as to protect the integrity of the thermocouple and to eliminate radiation effects from the flame. Since the temperature of the hot boundary was controlled by the heater, it was not changed during this flame-elimination process and was considered to be the ignition temperature when corrected for radiation losses according to Ref. [4]. The temperature measurements have an absolute uncertainty of ± 20 K due to uncertainties in the radiation correction and a relative error of ± 10 K, which represents errors in the individual measurements. Finally, to map the velocity field of the near-ignition state, the oxidizer temperature was reduced by 5–10 K below the ignition temperature and the fuel flow was restored before performing the LDV measurements.

Laminar ignition calculations were performed with the code of Kreutz and Law [5] with detailed transport and chemistry, using the reaction mechanism of Mueller et al. [11]. The calculations determined steady-state solutions at different hot boundary temperatures assuming potential flow. The ignition temperature was found by determining the boundary temperature at the lower turning point of the response S-curve.

Results and Discussion

Effects of Equivalence Ratio

To examine the effect of ϕ on ignition temperature, experiments and calculations were conducted at 1 atm and with a local strain rate of 390 s^{-1} . Results of the calculations for three equivalence ratios are shown in Fig. 1 in the form of S-curves, where the peak H atom concentration is plotted as a function of the hot boundary temperature. It is seen that as the boundary temperature is increased, the enhanced reaction rates lead to a gradual increase in

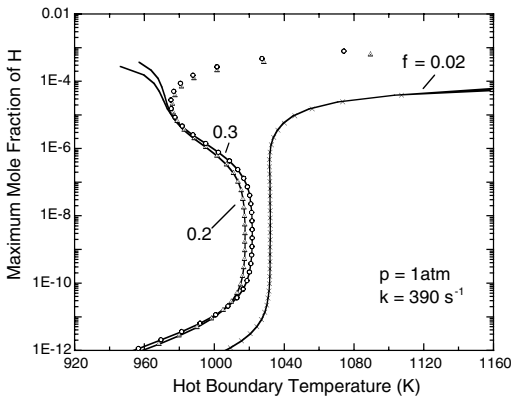


FIG. 1. Calculated S-curves for H_2 /air mixtures shown as solid line for three equivalence ratios. Symbols represent S-curves calculated with no heat release: circles for $\phi = 0.3$, triangles for $\phi = 0.2$, and crosses for $\phi = 0.02$.

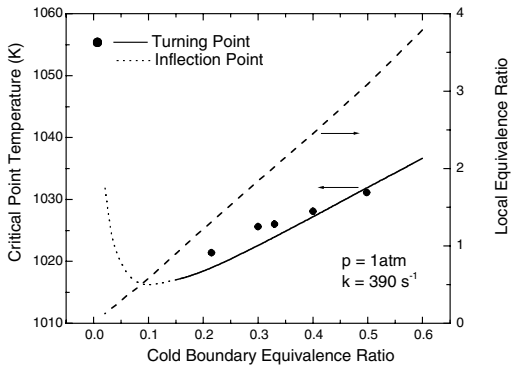


FIG. 2. Critical temperatures and local equivalence ratio as functions of boundary equivalence ratio. Experiments shown as symbols and calculations as solid line. Solid line represents turning points and dotted line represents inflection points.

the peak H concentration until a certain temperature is reached at which the reaction rates, and thus the H concentration, accelerate rapidly. When ϕ is not too small, such as in the $\phi = 0.2$ and $\phi = 0.3$ cases, the acceleration leads to a state of runaway characterized by a turning point. In these situations, the only solution at temperatures above the runaway temperature is on the flame branch (not shown) and the turning point identifies the ignition temperature. For very lean mixtures, say $\phi \approx 0.15$ for the present study, reaction rates are not sufficiently fast to cause a turning. An inflection point, followed by a gradual increase in H concentration, was observed and these flows are said to be unignitable.

The radical runaway can be caused by either pure kinetic acceleration or combined kinetic and thermal

acceleration triggered by heat release. In non-premixed ignitions, Kreutz et al. [2] found that, at pressures around the second limit, hydrogen ignites through pure radical runaway, without the need to consider thermal feedback. Similar results were seen in premixed stagnation ignition by Vlachos [12]. To investigate the nature of the ignition points in the present premixed counterflow, the calculations in Fig. 1 were repeated with the heat-release terms in the conservation equations suppressed; the results are plotted as symbols. It is seen that, for all equivalence ratios, the turning or inflection points are reproduced with negligible error without heat release, indicating that the reaction acceleration leading to ignition is purely kinetic in nature.

A final observation from Fig. 1 is the non-monotonic effect of ϕ on the ignition/inflection temperature, which decreases from $\phi = 0.02$ to $\phi = 0.2$ but increases again to $\phi = 0.3$. This issue is examined in more detail in Fig. 2 where the ignition/inflection temperature is plotted as a function of ϕ at the cold boundary, with the solid segment representing ignition temperatures, and the dotted segment the inflection temperatures. These calculated boundaries are compared with the experimental data, ranging from $\phi = 0.2$ to $\phi = 0.5$. Here, the lower boundary was determined by the weakest mixture for which the flame was sufficiently luminous to accurately identify the state of ignition, while the upper boundary was determined by the strongest mixture that could be stabilized experimentally, as discussed earlier. Very weak luminosity was actually observed down to $\phi = 0.15$, although such a state could not be determined precisely and hence is not indicated in Fig. 2. The quantitative agreement between calculation and experiment is within the experimental error, as specified earlier, and as such can be considered quite satisfactory. Qualitatively, the results show that the ignition temperature increases with increasing ϕ for the range of lean mixtures tested. This is surprising since the mixture reactivity is expected to be higher, and the ignition temperature lower, as ϕ approaches unity for the present lean mixtures.

The resolution to this interesting behavior comes by realizing that the equivalence ratio at the cold boundary does not directly indicate the mixture stoichiometry in the ignition kernel, and hence is not the most appropriate parameter to represent the system stoichiometry. To identify an appropriate stoichiometry for the phenomena, we plot in Fig. 3 the spatially resolved concentration profiles of T, H_2 , O_2 , and H for $\phi = 0.3$. It is seen that the ignition kernel, represented here by the H profile, lies on the hot side of the stagnation plane due to the Arrhenius dependence of reaction rates on temperature. This means that the reactants must diffuse across the stagnation plane before they can react in the kernel. Since fuel and oxidizer have different diffusivities,

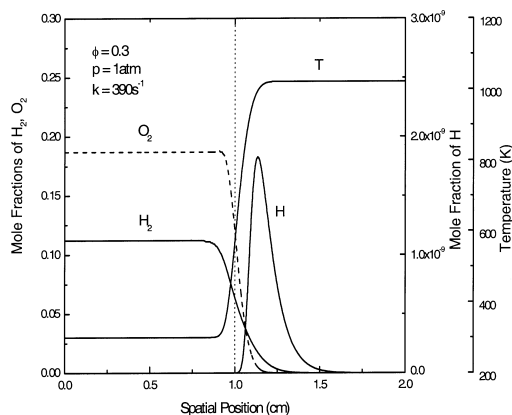


FIG. 3. Spatially resolved major (H_2 , O_2) and minor (H) species concentrations and temperature profiles.

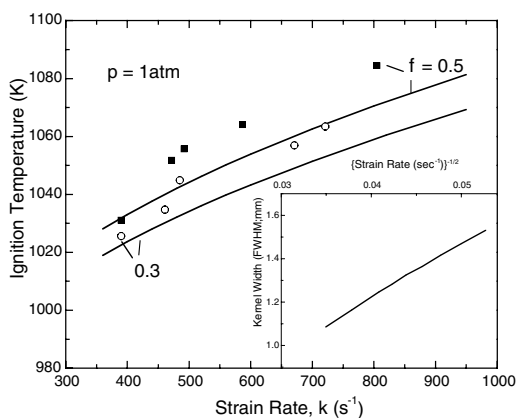


FIG. 4. Ignition temperatures at 1 atm as a function of strain rate. Experiments shown as symbols, and calculations shown as solid lines. The inset shows the dependence of the kernel width on the inverse of the square root of the strain rate.

the highly diffusive H_2 will penetrate much further into the hot side of the flow than the heavier O_2 , making the ignition kernel significantly richer than the reactant boundary. Fig. 3 shows that the hydrogen concentration is indeed significantly higher than the oxygen concentration in the ignition kernel. Since the most significant reaction rates are limited to the ignition kernel, the local ϕ , at the location of peak H concentration, is therefore more representative of conditions affecting ignition. Fig. 2 plots the local ϕ as a function of the boundary ϕ , and it is seen that the ignition kernel already becomes fuel rich when the boundary ϕ is 0.17. When the boundary ϕ is 0.5, the local ϕ is at a very rich value of 3.1. Since $\phi > 0.2$ in the present experimental study, the states of the ignition kernel are always fuel-rich.

Consequently, as the boundary ϕ becomes increasingly lean, the composition within ignition kernel becomes more stoichiometric, leading to higher reactivity and hence a lower ignition temperature. This explains the calculated and experimental results of Fig. 2.

Effects of Strain Rate

The effect of strain rate on premixed ignition temperatures was examined at 1 atm and two different equivalence ratios. The experimental results, shown in Fig. 4, exhibit the same trends as the calculations, which fall within the measurement accuracy. The calculated kernel width is found to scale with the inverse square root of the strain rate, as shown in the inset of Fig. 4. The resulting decrease in the residence time as the kernel width becomes smaller is the reason that the ignition temperature increases with strain rate, similar to non-premixed ignition [5]. It is of particular interest to note that, compared with non-premixed ignition at the same pressure, the premixed ignition temperatures are much higher and the dependence on strain rate is more pronounced. Both observations are significant departures from the second ignition limit behavior seen in non-premixed ignition at 1 atm where the ignition temperature lies close to the crossover temperature. In that limit, the key elementary reaction rates are orders of magnitude faster than convection and diffusion rates, thereby rendering ignition only weakly sensitive to changes in strain rate. In contrast, the increased dependence of ignition temperature on strain rate in premixed ignition is qualitatively similar to non-premixed ignition in the first limit, where the reactions are slowed to the point that diffusive rates are of the same order as kinetic rates. Radical loss due to transport processes becomes competitive with chain termination, hence hindering ignition and rendering it sensitive to changes in residence time as the strain rate is varied.

The increased importance of diffusion relative to chemical reaction for premixed ignition is illustrated in Fig. 5 by comparing the spatially resolved reaction and transport rates. It is seen that, in contrast to non-premixed ignition, the rates of individual H atom production and consumption reactions (Fig. 5a) in premixed ignition are of the same order of magnitude as that for the diffusive loss (Fig. 5b). This diffusive loss is indicated by the relatively long tail of its concentration profile (Fig. 3) that lies almost entirely outside of the region of the peak reaction rates. Since a minimum radical pool is needed for kinetic runaway to occur, higher ignition temperatures are thus needed such that chemical production can overcome the transport loss.

Effects of O_2 Addition to Hot Boundary

The role that the absence of oxygen in the hot flow plays in increasing the relative amount of diffusive

FIG. 8. Spatially resolved rates for hydrogen radical production, destruction, and mass transport (mole $\text{cm}^{-3} \text{s}^{-1}$) at 1 atm, $k = 390 \text{ s}^{-1}$. (Left) Rates of individual elementary reactions. (Right) Rates of diffusive and convective transport compared with the overall chemical production rate. (a and b) partially premixed case (fuel side, $\phi = 0.3$; hot side, 1% O_2 in N_2). (c and d) non-premixed case (fuel side, 11.2% H_2 in N_2 ; hot side, air).

the critical radical concentration to build up at a temperature that is about 70 K lower than the premixed case. Finally, the saturation effect is indicated by the fact that the 1% O_2 profile is somewhat wider but otherwise qualitatively similar to the non-premixed profile.

More details of the effect of O_2 addition on ignition can be identified by comparing the reaction and transport rate profiles. The premixed reaction rate profiles shown in Fig. 5a are narrow, lie close to the stagnation plane, and are of nearly the same magnitude as the diffusion rates shown in Fig. 5b. All of these observations reflect the slow reaction rates in the oxygen-starved kernel and the increasingly rich conditions from preferential diffusion when moving away from the stagnation location into the hot flow. Fig. 8 compares the reaction and transport profiles for the non-premixed flow and premixed flow with 1% O_2 addition. When O_2 is added to the hot flow, the reaction rate profiles at ignition, shown in Fig. 8a, become wider and move away from stagnation as oxidizer becomes available in the high-temperature region. By reducing the relative influence of diffusion and the resultant broadening, the wider reaction profiles are responsible for the narrower species profiles noted in Fig. 7. The peak reaction rates are larger than the diffusion rates in Fig. 8b by about a factor of 3, indicating that the effect of diffusion relative to reaction is weaker than in the purely premixed flow. As a result, the radical pool is able to be established more readily, the kernel is narrower, and the ignition temperature is lowered. In the non-premixed flow, reaction rates in Fig. 8c are an order of

magnitude higher than the diffusion rates in Fig. 8d, reflecting the insensitivity to transport effects characteristic of the second ignition limit. The location of the peak reaction rates is the same as for the premixed case with O_2 addition, indicating that the oxidizer deficiencies affecting ignition in premixed flows are eliminated with only 1% O_2 added to the inert flow and that further oxygen addition increases reaction rates but does not produce any qualitative changes.

Concluding Remarks

The ignition of lean premixed hydrogen/air by hot nitrogen was studied in a laminar counterflow over a range of equivalence ratios and strain rates. Ignition temperatures were found to decrease when the mixture ϕ decreased down to 0.2. The ignition kernel is located on the hot side of the flow and is formed by the diffusion of fuel and oxidizer from the reactant side. The large diffusivity difference between H_2 and O_2 results in varying concentrations in the hot flow, with the more diffusive H_2 being relatively enriched. As a result, the ignition kernel is much richer than the initial reactant mixture. When the boundary equivalence ratio becomes leaner, the local equivalence ratio in the kernel moves toward stoichiometric, the mixture reactivity increases, and the ignition temperature decreases.

One of the consequences of the oxygen-deprived kernel is that reaction rates decrease to the point where diffusive transport of the H atom from the

kernel becomes important. The diffusive loss is most pronounced on the hot side of the kernel because the increasingly rich mixture reduces reaction rates further, resulting in a tail to the H concentration profile toward the hot boundary. Since the diffusive transport is similar in magnitude to the chain-terminating reactions, premixed ignition temperatures are typically 80 K higher than nonpremixed ignition temperatures and are more sensitive to changes in strain rate.

The dearth of oxidizer in the ignition kernel can be addressed by adding small amounts of oxygen to the hot nitrogen. Ignition temperatures approach non-premixed values by adding as little as 1% O₂ to N₂ and further oxygen addition has little effect. By increasing reaction rates and reducing diffusive loss, the premixed kernel with oxygen addition becomes similar to the non-premixed kernel even though the total amount of oxidizer is different. This provides an important link between premixed and non-premixed ignition. In practical situations, it is reasonable to expect that some amount of oxidizing species would be present in the hot flow, perhaps as a result of lean combustion or the dissociation of combustion products, and the scenario of premixed ignition with oxidizer doping is a possibility that needs to be considered.

The unique features identified for premixed hydrogen/air ignition in the counterflow are derived from the high diffusivity of hydrogen relative to air, suggesting that the effects would be minimized if the diffusivity of the fuel is similar to that of oxygen or reversed if the fuel is much heavier than oxygen, for example, heptane and dodecane. In the latter case, oxygen is the faster moving species and, consequently, adding fuel to the hot inert side of the flow could potentially enhance ignition. Finally, these unique features are suppressed when the heated inert jet is replaced by a hot surface, eliminating the

process of preferential diffusion across the permeable interface and the resulting concentration stratification.

Acknowledgments

This work was primarily sponsored by the Army Research Office under the technical monitoring of Dr. D. Mann. T.G.K. was supported by a block grant from the British Petroleum Corp. to the Center for Carbon Mitigation Initiative at Princeton University.

REFERENCES

1. Darabiha, N., and Candel, S., *Combust. Sci. Technol.* 86:67–85 (1992).
2. Kreutz, T. G., Nishioka, M., and Law, C. K., *Combust. Flame* 99:758–766 (1994).
3. Balakrishnan, G., Smooke, M. D., and Williams, F. A., *Combust. Flame* 102:329–340 (1995).
4. Fotache, C. G., Kreutz, T. G., Zhu, D. L., and Law, C. K., *Combust. Sci. Technol.* 109:373–394 (1995).
5. Kreutz, T. G., and Law, C. K., *Combust. Flame* 104:157–175 (1996).
6. Kreutz, T. G., and Law, C. K., *Combust. Flame* 114:436–456 (1998).
7. Fotache, C. G., Sung, C. J., Sun C. J., and Law, C. K., *Combust. Flame* 112:457–471 (1998).
8. Sung, C. J., and Law, C. K., *Combust. Sci. Technol.* 129:347–360 (1997).
9. Blouch, J. D., Sung, C. J., Fotache, C. G., and Law, C. K., *Proc. Combust. Inst.* 27:1221–1228 (1998).
10. Vlachos, D. G., Schmidt, L. D., and Aris, R., *Combust. Flame* 95:313–335 (1993).
11. Mueller, M. A., Kim, T. J., Yetter, R. A., and Dryer, F. L., *Int. J. Chem. Kinet.* 31:113–125 (1998).
12. Vlachos, D. G., *Combust. Flame* 103:59–75 (1995).